Comparative Inter-Laboratory Study of Wind Loading on Low Industrial Buildings

by

Bogusz Bienkiewicz[1], Munehito Endo[1], Joseph A. Main[2], and William P. Fritz[3]

ABSTRACT

Results of an ongoing inter-laboratory comparative study of approach flow and wind pressures on low buildings are presented. The wind tunnel data generated at six wind engineering laboratories during a pilot project initiated and coordinated by the National Institute of Standards and Technology was employed. Variability in the laboratory wind loading on low buildings was investigated. The largest variability in the laboratory wind pressures and in the associated wind-induced internal loading in structural frames of generic low buildings was found for suburban wind exposure, for which an average coefficient of variation of 26.6 % was observed. This variability was primarily attributed to differences in the approach flows employed in physical modeling of wind pressures on tested buildings, carried out by the participating laboratories. The variability in the approach flows resulted in a large measure from the differences in the along-wind turbulence intensity implied by different empirical models, defining the target wind exposures and used by the laboratories.

KEYWORDS: wind loading, low buildings, wind tunnel testing

1.0 INTRODUCTION

The consistency of wind loading on low buildings inferred from wind tunnel testing has been of concern to wind engineering researchers and practitioners, structural engineers and code writers. The National Institute of Standards and Technology (NIST) has initiated and coordinated a pilot project addressing this issue. Two representative low buildings of rectangular plan and two wind exposures were selected for the study and a number of wind engineering laboratories were invited to carry out wind tunnel testing to determine wind loading on the buildings.

To ensure consistency in laboratory settings, most of the experimental conditions were specified by the coordinating team at NIST. They included: geometrical scale, data sampling rate and record length, number of data records and locations of pressure taps. Ultimately, six laboratories (four from North America, one from Japan and one from Europe) provided datasets, of which a total of seven have been deposited at and analyzed by NIST. These sets consisted of time series and statistical summaries of coefficients of external pressure acquired at specified taps. Information on modeling and statistical properties of approach wind was also provided.

The above data were employed in calculations of internal forces (bending moment, shear force, etc.) in representative frames of metal buildings of geometry modeled in the wind tunnel tests, Fritz et al. [1]. The results of this analysis indicated large differences in the forces calculated using the datasets generated at different laboratories. The largest variability was found for a building of a relatively low height (a prototype eave height of 6.1 m), placed in the suburban wind exposure, Fritz et al. [1]. These discrepancies were tentatively attributed to a number of experimental factors and assumptions made during wind tunnel testing.

[1] Wind Engineering and Fluids Laboratory, Department of Civil and Environmental Engineering, Colorado State University, Fort Collins, CO 80523-1320, USA

[2] Building and Fire Research Laboratory, National Institute of Standards and Technology, Gaithersburg, MD 20899-8611, USA

[3] Wells Fargo Bank, Columbia, MD 21046, USA (formerly, Building and Fire Research Laboratory, National Institute of Standards and Technology)

However, it has been recognized that a systematic investigation would be required to provide definite explanation of the origins of this variability and to develop means to reduce/eliminate these discrepancies. The overall objective of the paper is to present a progress report on an ongoing collaborative study addressing the above variability, its origins and related issues.

2.0 BUILDINGS AND TEST SETUP

The two buildings selected for the inter-laboratory study, see Figure 1, had the same planar dimensions, 30.5 m by 61 m, and the same slope of the gable roof, 2.39° (1/2 in 12). The main difference between the buildings was the eave height: 6.1 m and 9.8 m.

Selection of the pressure tap locations was based on a layout developed by the Boundary Layer Wind Tunnel Laboratory, at the University of Western Ontario, for wind tunnel testing carried out as part of the NIST/Texas Tech University Windstorm Mitigation Initiative. In view of varying capabilities – number of data channels of pressure measurement systems available at different laboratories – a subset of that layout (comprising of a smaller number of taps) was chosen and assigned to the laboratories participating in this study. The selected taps were located in rows 1 through 5, as is schematically depicted in Figure 1.

3.0 RESULTS

The primary focus of the investigation presented in the paper was an inter-laboratory comparison of the modeled approach flows, acquired building point pressures and the wind-induced internal forces (bending moments) computed in main wind force resisting system (MWFRS). The considered system (MWFRS) is shown in Figure 2. This system was also employed by Whalen et al. [2], in investigation of wind-induced internal forces. In the present structural analysis, the frame geometry was simplified, as is depicted in Figure 3, and the influence lines were employed in calculations. Coefficients α and β were used to control respectively the frame stiffness and aspect ratios. Representative results of this effort are presented herein. Letter labeling – A through F – is used to denote the source (participating laboratories) of the compared approach wind, wind-induced external point pressure and other referenced information provided by the laboratories. While uncertainty estimates were not provided by each laboratory, estimates based on repeated tests from one particular laboratory indicate a coefficient of variation (COV) of approximately 2 % in the mean wind speed and a COV of approximately 3 % in the mean and standard deviation of pressure coefficients. Error bars are not shown in figures as they are smaller than the plotting symbols.

Regarding the approach flow, it was found that significantly different experimental set-ups were used by the laboratories to simulate a given target wind exposure. This is illustrated in Figure 4, where the wind tunnel configurations employed to generate the suburban wind exposure at three representative laboratories (denoted A, B and C) are displayed. For this exposure, the experimental setups were found to exhibit the largest differences.

The impact of the differences in the setups depicted in Figure 4 can be inferred from Figures 5 and 6, where the vertical profiles of the along-wind mean velocity and turbulence intensity are displayed, for the two approach flows modeled at four representative laboratories. As can be seen in Figure 5, the inter-laboratory discrepancy in the mean velocity profiles is moderate, with the power-law exponents ranging from 0.139 through 0.191 (target value of 0.143) and from 0.165 through 0.234 (target value of 0.22) for the open and suburban wind exposures, respectively. It can be seen in Figure 6 that the spread among the compared turbulence intensity profiles is significantly larger. The largest discrepancy is observed for the (modeled) suburban exposure.

It should be pointed out that the participating laboratories used different empirical models to define the target profiles for the approach flows modeled in boundary-layer wind tunnels. Representative comparisons of these models are depicted in Figure 7 and they include: ASCE 7 [3], Eurocode [4], AIJ [5], AS1170.2 [6] and NBCC [7] (from Zhou and Kareem [8]), and two variants of ESDU model (from [9] and [10]). It can be seen

that the spread in these profiles is overall similar to that exhibited by the profiles of the simulated (laboratory) approach flows, shown in Figure 6.

Representative wind-induced mean roof pressures at tap rows 1 through 3 (compare Figure 1), acquired at five or six (one case) laboratories are depicted in Figure 8. The resulting wind-induced mean bending moments in frame F1 (compare Figure 2), normalized by the square of the rooftop mean velocity, are shown in Figure 9. Overall, the displayed mean roof pressures and the bending moments show similar trends. A comparison of the results originating from different laboratories reveals a scatter among the data, which is primarily attributed to the level of turbulence of the modeled approach flows. It can be seen in Figure 8 that the highest level of the inter-laboratory discrepancy occurred in suburban exposure – the exposure that exhibited the largest discrepancy in the turbulence intensity of the modeled approach flow, see Figure 6. A similar trend, although the magnitude of the inter-laboratory discrepancy is lower, can be observed for the bending moments, in Figure 9.

The time series of the roof pressures and bending moments were subsequently employed to predict the peak pressures and bending moments. The peak estimation procedure proposed by Sadek and Simiu [11] was employed in this analysis. Representative results are presented in Figures 10 and 11, for suburban approach flow. The 90th percentile pressure peaks at two locations in a roof corner region (taps P1 and P2 in Figure 1) are displayed in Figure 10. The 90th percentile peak bending moments in two frames (frames F1 and F2 in Figure 2) are shown in Figure 11.

The data depicted in Figures 10 and 11 indicate significant inter-laboratory scatter in the peak wind loading and the resulting internal force (bending moment). This variability is quantified in Figures 12 and 13, using the coefficient of variation (COV). It can be seen that the COV computed for suburban exposure is significantly larger than that for open exposure. The overall COV of roof pressures and bending moments are compared in Table 1 with the COV of turbulence intensity.

The results in Table 1 show that in open exposure the inter-laboratory variability in the roof pressure and the frame bending moment was moderate, with the average coefficient of variation of approximately 13 % for the building of lower height (6.10 m) and 10 % for the building of larger height (9.75 m). The variability was approximately twice as large in suburban exposure. This increase can be attributed to an increased variability in the turbulence level (turbulence intensity) displayed in Table 1. It is postulated that the inter-laboratory variability in the internal loading reported by Fritz et al. [1] is in a large measure caused by the variability in the approach flow turbulence employed in physical modeling of wind pressure on tested buildings, carried out by the participating laboratories.

4.0 CONCLUDING REMARKS

Results of an ongoing inter-laboratory comparative study of approach flow, wind pressures on low buildings and internal wind-induced loading are presented. The largest variability in the laboratory wind pressures and in the associated (computed) wind-induced internal loading (bending moment) in structural frames of generic low buildings was found for suburban wind exposure. This variability was primarily attributed to differences in the approach flows employed in physical modeling of wind pressures on tested buildings, carried out by the participating laboratories. The variability in the approach flows resulted in a large measure from the differences in the along-wind turbulence intensity implied by different empirical models, defining the target wind exposures and used by the laboratories. A follow-up comparative inter-laboratory study is planned to address a number of issues identified in the ongoing efforts.

5.0 ACKNOWLEDGEMENTS

The authors would like to express gratitude to Dr. E. Simiu of the National Institute of Standards and Technology for initiating and managing the inter-laboratory wind tunnel project and for his contributions to the ongoing investigation. All of the participants in the inter-laboratory comparative

study are gratefully acknowledged, including Bo Cui of the Clemson Wind Load Test Facility at Clemson University; Olivier Flamand of the Centre Scientifique at Technique du Bâtiment (CSTB) in Nantes, France; Eric Ho of the Boundary Layer Wind Tunnel Laboratory at the University of Western Ontario; Hitomitsu Kikitsu of the Building Research Institute in Tsukuba, Japan; and Chris Letchford of the Wind Science and Engineering Research Center at Texas Tech University.

6.0 REFERENCES

[1] W.P. Fritz, B. Bienkewicz, O. Flamand, E. Ho, H. Kikitsu, C.W. Letchford, and C. Bo, International comparison of wind tunnel estimates of wind effects on an industrial building model: test-related uncertainties, UJNR, Proc. The 4th U.S.-Japan Workshop on Wind Engineering, July 20-22, Tsukuba, Japan, 2006, 12 pp.

[2] T. Whalen, E. Simiu, G. Harris, J. Lin, and D. Surry, The use of aerodynamic database for the effective estimation of wind effects in main wind-force resisting systems: application to low buildings, J. Wind Eng. Ind. Aerodyn. 77&78 (1998) 685-693.

[3] ASCE 7-02, Minimum Design Loads for Buildings and Other Structures, American Society of Civil Engineers, New York, USA, 2002.

[4] Eurocode, Eurocode 1: Basis of Design and Actions on Structures. Part 2-4: Actions on Structures–Wind Actions, European Prestandard, ENV-1991-2-4, 1995.

[5] AIJ, Recommendations for Loads on Buildings, Architectural Institute of Japan, Tokyo, Japan, 1996.

[6] AS1170.2, Australian Standards: SAA Loading Code, Part2 – Wind Loads, AS1170.2-89, Australia, 1989.

[7] NBCC, Commentary B–Wind Loads, User's Guide-NBC 1995 Structural Commentaries, Canadian Commission on Building and Fire Codes, National Research Council of Canada, Ottawa, Canada, Part 4, 9-42, 1996.

[8] Y. Zhou, A. Kareem, Definition of wind profiles in ASCE 7, J. Struct. Engrg. 128 (8) (2002) 1082-1086.

[9] T.C.E. Ho, D. Surry and D. Morrish, NIST/TTU Cooperative Agreement – Windstorm Mitigation Initiative: Wind Tunnel Experiments on Generic Low Buildings, Tech. Rep. BLWT-SS20-2003, The Boundary Layer Wind Tunnel Laboratory, The University of Western Ontario, London, Ontario, Canada, May 2003, 105 pp.

[10] O. Flamand, Measurement of time series of pressures on a low-rise building for the NIST, Tech. Rep. ENCAPE 03.146 C-V0, CSTB, Nantes, France, 2003, 12 pp.

[11] F. Sadek and E. Simiu, Peak non-Gaussian wind effects for database-assisted low-rise building design, J. Eng. Mech. 128 (5) (2002) 530-539.

Table 1. Overall inter-laboratory variability of approach flow, point pressure and frame bending moment

Building height (m)	Exposure (O=open S=Suburban)	Turbulence intensity (%)					COV (%) for Cp (peak) [Cp (mean)]		COV (%) for M1 (peak) [M1 (mean)]		Average COV (%)
		Max ($\hat{M}$)	Mean	Min ($\check{M}$)	Δ ($\hat{M}-\check{M}$)	COV	Tap P1	Tap P2	Frame F1	Frame F2	
6.10	O	21.1	19.8	18.2	2.9	6.2	16.5 [11.7]	11.6 [9.0]	14.7 [12.7]	21.3 [15.7]	14.2
6.10	S	31.2	27.4	24.9	6.4	9.9	25.8 [33.7]	22.9 [21.3]	21.9 [31.6]	21.7 [45.2]	28.0
9.75	O	20.7	18.8	16.7	4.0	10.1	20.4 [8.8]	10.4 [8.4]	13.7 [5.9]	13.1 [7.5]	11.0
9.75	S	32.4	27.0	23.8	8.6	13.8	26.9 [31.3]	24.3 [19.7]	24.6 [23.4]	22.2 [29.5]	25.2

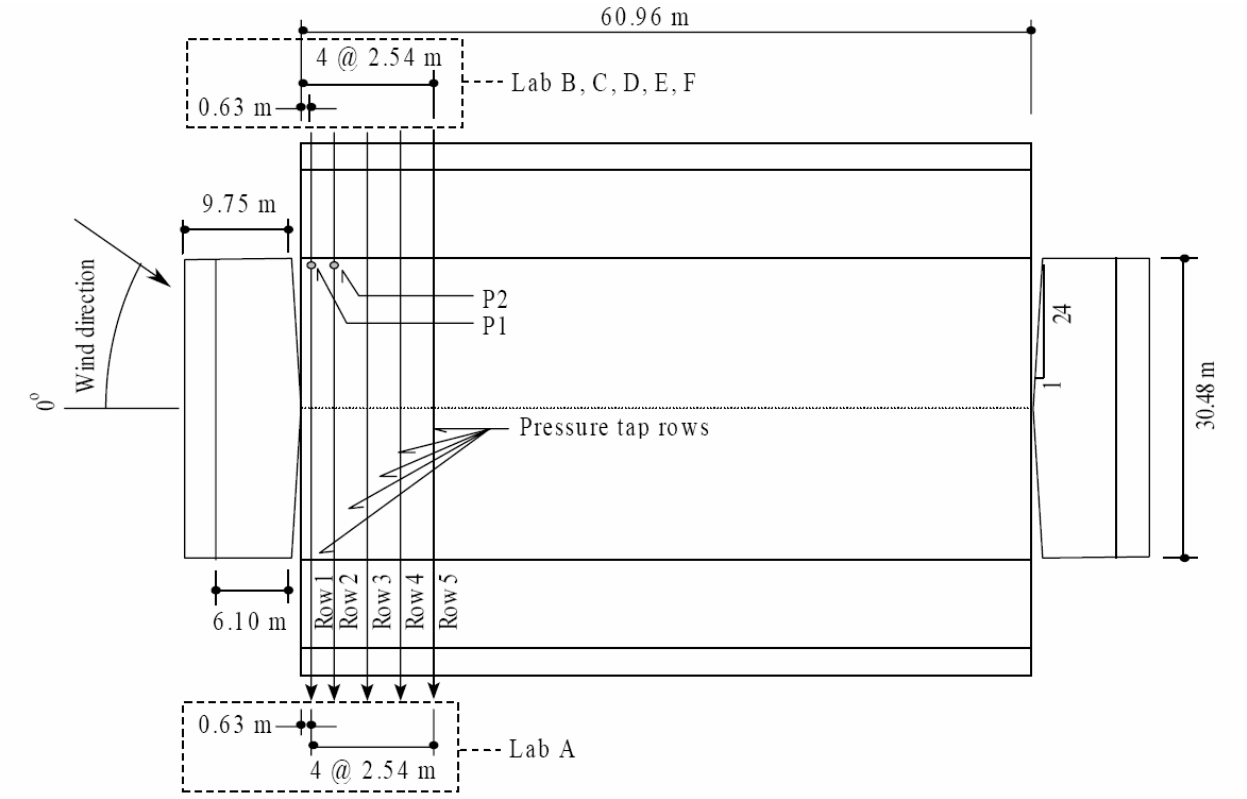

Figure 1. Geometry of prototype low buildings and pressure tap locations.

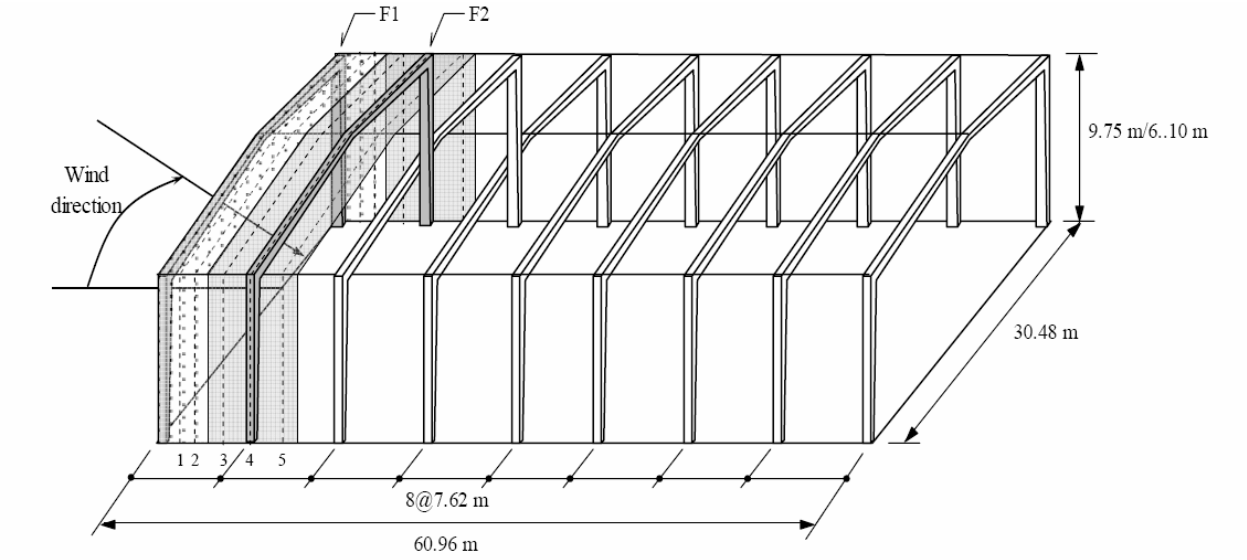

Figure 2. Geometry and main wind force resisting system (MWFRS) of low building.

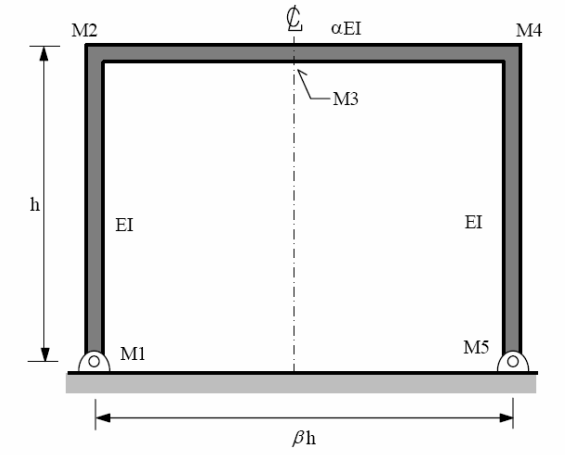

Figure 3. Simplified geometry of structural frame.

Figure 4. Wind tunnel setups to generate suburban wind exposure in three representative laboratories.

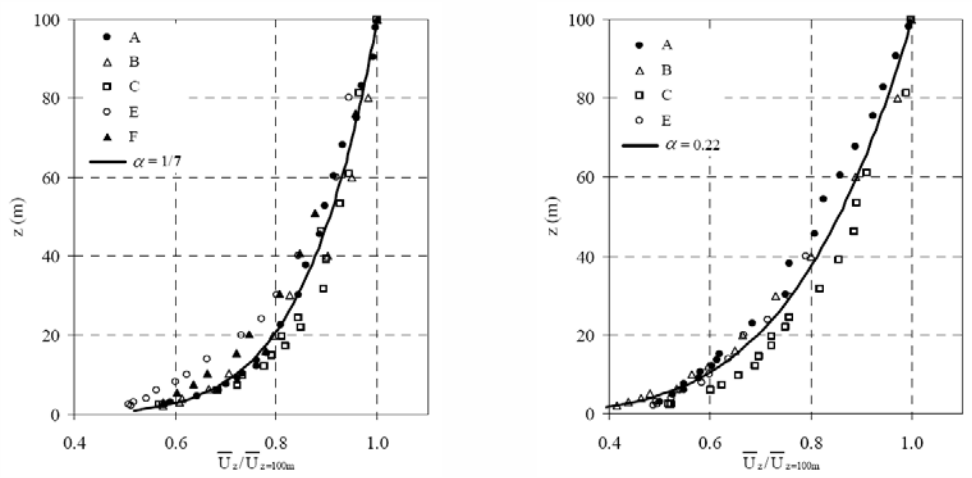

(a) Open exposure (b) Suburban exposure

Figure 5. Comparison of laboratory and target mean wind speed profiles.

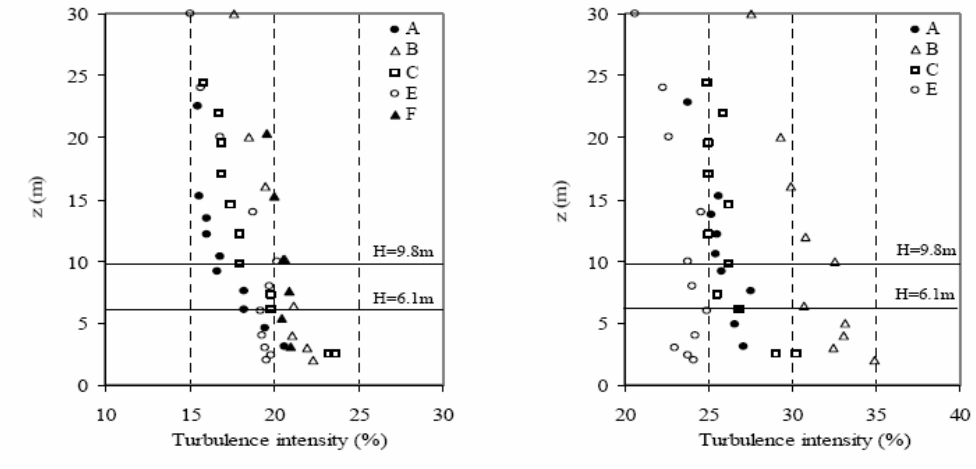

(a) Open exposure (b) Suburban exposure

Figure 6. Comparison of laboratory along-wind turbulence intensity profiles

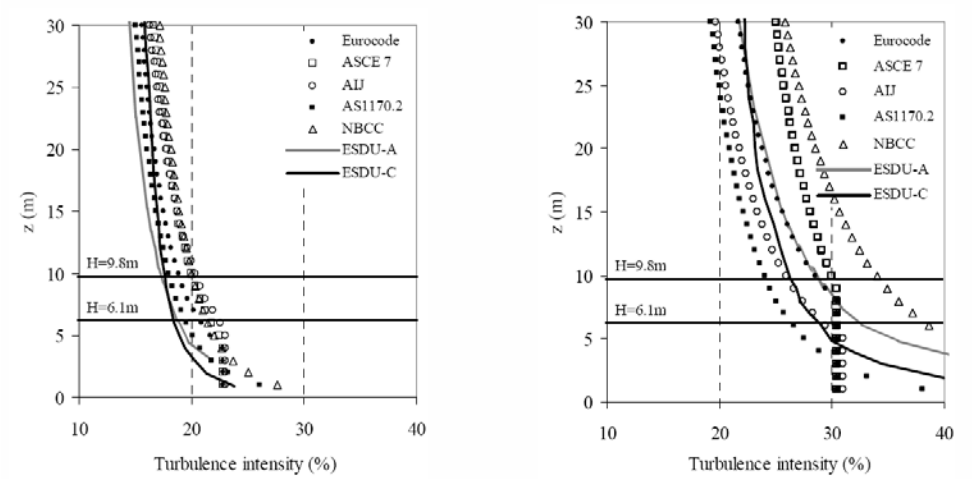

(a) Open exposure (b) Suburban exposure

Figure 7. Comparison of empirical models for along-wind turbulence intensity profiles.

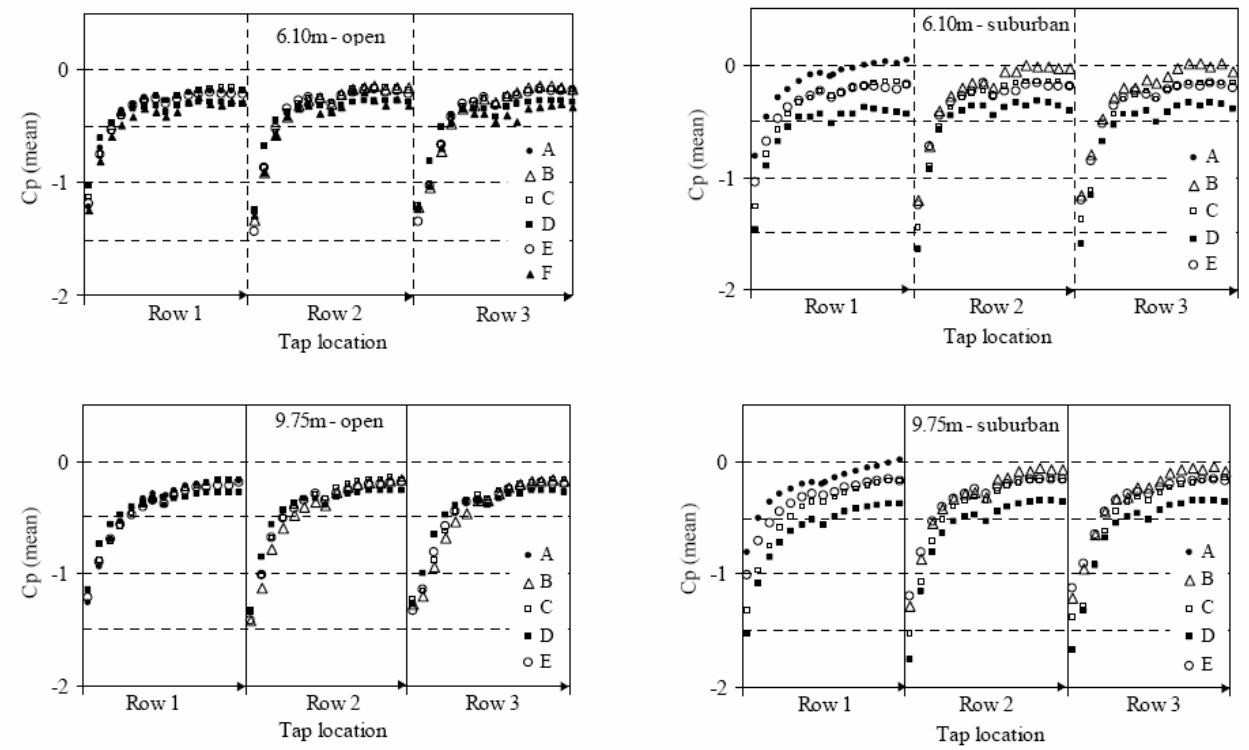

Figure 8. Representative mean roof pressure coefficient, wind normal to ridge (wind direction 90°).

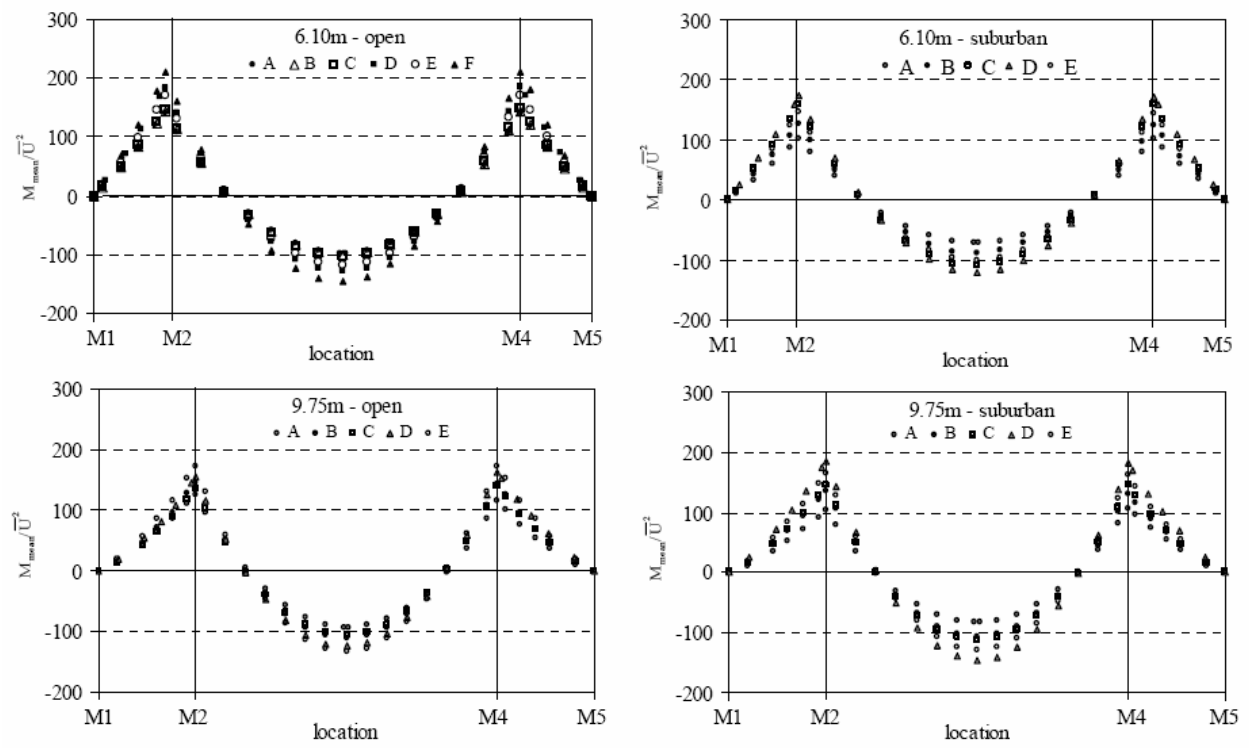

Figure 9. Mean bending moment in frame F1, wind parallel to ridge (wind direction 0°).

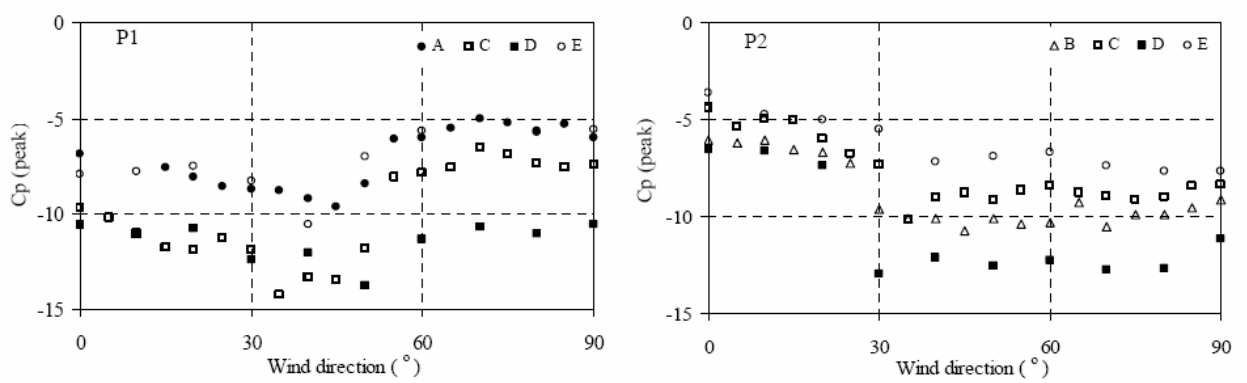

Figure 10. The 90th percentile roof peak pressure, building height 6.10 m, suburban exposure.

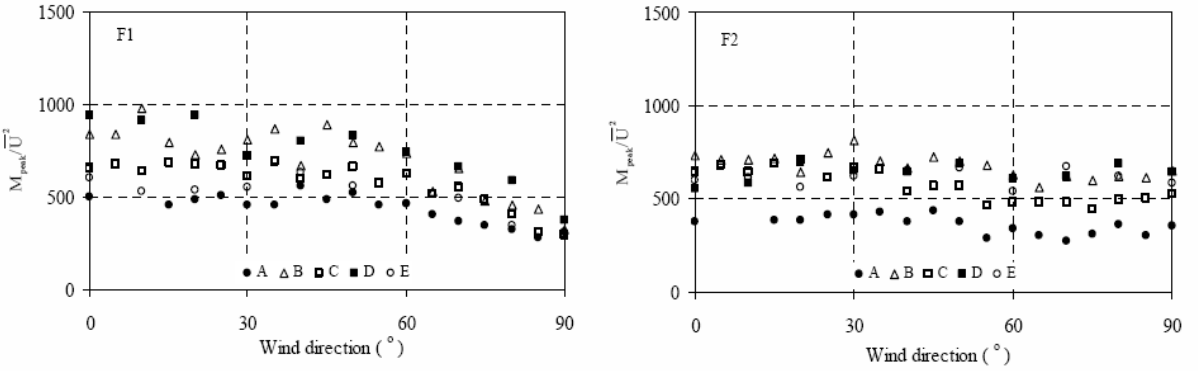

Figure 11. The 90th percentile peak bending moment, location M2, building height 6.1 m, suburban exposure.

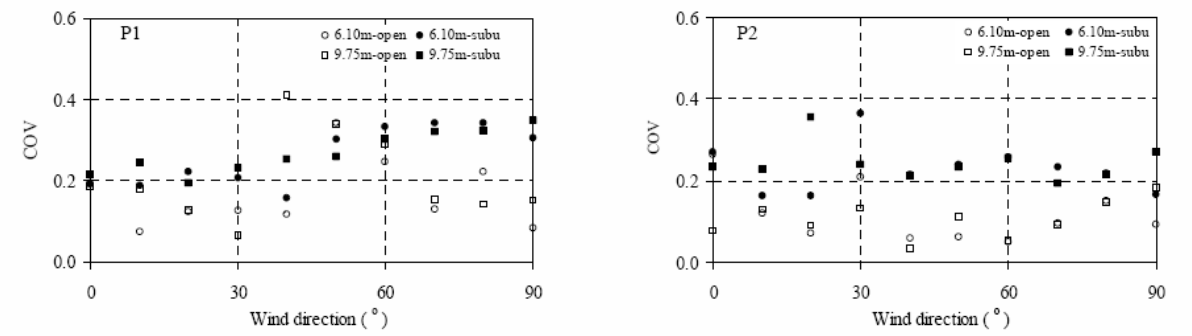

Figure 12. Comparison of COV for 90th percentile peak pressure.

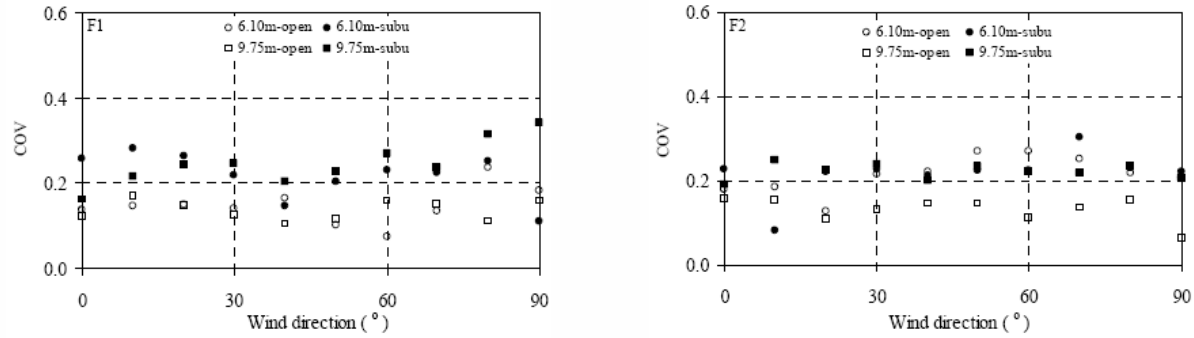

Figure 13. Comparison of COV of 90th percentile peak bending moment, location M2.